Journal of Magnetic Resonance **152,** 79–86 (2001)
doi:10.1006/jmre.2001.2389, available online at http://www.idealibrary.com on IDEAL®

Characterization of the Effects of Nonspecific Xenon–Protein Interactions on ^{129}Xe Chemical Shifts in Aqueous Solution: Further Development of Xenon as a Biomolecular Probe

Seth M. Rubin,* Megan M. Spence,† Alexander Pines,† and David E. Wemmer*,[1]

*Department of Chemistry, University of California, Berkeley, California 94720; and *Physical Bioscience and †Material Sciences Divisions, Lawrence Berkeley National Laboratory, Berkeley, California 94720*

Received December 19, 2000; revised April 25, 2001; published online August 1, 2001

The sensitivity of ^{129}Xe chemical shifts to weak nonspecific xenon–protein interactions has suggested the use of xenon to probe biomolecular structure and interactions. The realization of this potential necessitates a further understanding of how different macromolecular properties influence the ^{129}Xe chemical shift in aqueous solution. Toward this goal, we have acquired ^{129}Xe NMR spectra of xenon dissolved in amino acid, peptide, and protein solutions under both native and denaturing conditions. In general, these cosolutes induce ^{129}Xe chemical shifts that are downfield relative to the shift in water, as they deshield the xenon nucleus through weak, diffusion-mediated interactions. Correlations between the extent of deshielding and molecular properties including chemical identity, structure, and charge are reported. Xenon deshielding was found to depend linearly on protein size under denaturing solution conditions; the denaturant itself has a characteristic effect on the ^{129}Xe chemical shift that likely results from a change in the xenon solvation shell structure. In native protein solutions, contributions to the overall ^{129}Xe chemical shift arise from the presence of weak xenon binding either in cavities or at the protein surface. Potential applications of xenon as a probe of biological systems including the detection of conformational changes and the possible quantification of buried surface area at protein–protein interfaces are discussed.

Key Words: **xenon NMR; ^{129}Xe chemical shifts; xenon–protein interactions; biomolecular probes.**

INTRODUCTION

Following initial studies of xenon in porous solids (*1*) xenon NMR spectroscopy has become a promising technique for probing molecular structure and dynamics in materials, liquids, and molecules in solution (*2–5*). The magnetic resonance properties of ^{129}Xe are extremely sensitive to its local chemical environment and large ^{129}Xe NMR signals are readily attainable through the use of established optical pumping techniques (*6*). The relatively small size and hydrophobicity of xenon make it well suited for probing biological systems in aqueous solution. The ^{129}Xe chemical shift undergoes dramatic changes upon specific binding to the nonpolar interiors of proteins and structured lipids (*7–11*). In addition, it has recently been reported that even weak nonspecific interactions between xenon and protein surfaces have a measurable effect on the chemical shift of xenon and that this effect changes upon protein denaturation (*12–13*). This sensitivity of the ^{129}Xe chemical shift to neighboring chemical composition and structure could make xenon a reporter of biomolecular conformations and interactions and their changes with varying solution conditions. However, detailed interpretation of NMR data of xenon in biological systems remains difficult given the limited understanding of the influence of different chemical environments on the ^{129}Xe chemical shift in aqueous solution. Because not all macromolecules bind xenon with high affinity, knowledge of how nonspecific xenon–macromolecule interactions affect the ^{129}Xe chemical shift is particularly important for the development of xenon as a general biomolecular probe.

Previous studies of how chemical environments in gases, liquids, and solids influence ^{129}Xe chemical shifts provide a foundation for the understanding of the effects of xenon–protein interactions. The large range of ^{129}Xe chemical shifts (over 5000 ppm) is due to the polarizability of its large electron cloud which shields the nucleus from the surrounding magnetic field (*2–5*). In the gas phase, interatomic collisions distort the xenon electron cloud so that the nucleus becomes deshielded and the ^{129}Xe resonance frequency shifts downfield continuously with increased gas density (*14*); for clusters of xenon gas trapped in porous solids, this downfield shift is discrete and depends on cluster size (*15*). The chemical shift of ^{129}Xe in solution can be up to several hundred ppm downfield of the frequency of xenon in the gas phase; this deshielding effect is dominated by dispersive van der Waals interactions between the dissolved noble gas and solvent molecules (*7, 16–18*). Some accounts of the van der Waals contribution have treated the solvent as a continuum that produces an electric field in response to electronic fluctuations of the xenon (*7, 19*). Studies of xenon in *n*-alkanes and

[1] To whom correspondence should be addressed, E-mail: dewemmer@LBL.gov.

1090-7807/01 $35.00

various linear, functionalized hydrocarbons have led to a more discrete molecular description of ^{129}Xe NMR solvent shifts in which the overall deshielding is treated as a sum of deshielding effects arising from pair interactions between xenon and functional groups on solvent molecules (*17, 18*). Theoretical calculations have confirmed that ^{129}Xe chemical shifts in solvents can be correlated with pairwise summations of solute–solvent dispersive interaction energies using molecular pair distribution functions (*20*).

Both reaction field and group contribution analyses of solvated xenon chemical shifts fail to predict the ^{129}Xe shift in water, where deshielding is about 45 ppm greater than expected (*7*). This discrepancy is likely due to a unique water structure around the nonpolar xenon solute. The presence of such structural effects in liquid water is anticipated by ^{129}Xe NMR spectroscopy of xenon in clatherate hydrates (*21*). These studies have revealed the existence of small and large water cages in which ^{129}Xe resonance frequencies are ≈240 and ≈150 ppm downfield from the gas phase, respectively. An understanding of how cavity structure affects ^{129}Xe chemical shifts is provided by experiments on xenon trapped in clathrates, zeolites, and nanochannels (*22–24*). For example, the deshielding of xenon increases with decreasing cavity size and depends on the shape of the cavity due to its influence on the anisotropy of the electron cloud of xenon. Such structural effects likely influence the chemical shifts of xenon interacting both specifically and nonspecifically with macromolecules and other solutes in aqueous solution.

Several previous studies have detected effects of nonspecific xenon–solute interactions in water on ^{129}Xe chemical shifts. In solutions of metal cations and halide anions, diffusion-mediated interactions lead to a downfield shift relative to water that increases linearly with increasing salt concentration (*25*). The concentration-normalized chemical shift (here denoted α and expressed in units of ppm/mM) increases with ion charge, corresponding to a greater polarization of the xenon electron cloud. ^{129}Xe chemical shifts in solutions of oligosaccharides derived from glucose have been reported with α values ranging from 0.006 ppm/mM downfield for the monomer to 0.038 ppm/mM downfield for maltohexose (*26*). Nonspecific interactions between xenon and metmyoglobin under both native and denaturing solution conditions also induce downfield ^{129}Xe shifts relative to the ^{129}Xe shift in water (*13*). These interactions have been modeled as weak binding sites such that, in the limit where a small fraction of xenon is bound to nonspecific sites,

$$\alpha = \sum_{\text{nonspecific sites}} \delta_{\text{nonspecific}} K_{\text{nonspecific}}, \qquad [1]$$

where $\delta_{\text{nonspecific}}$ is the chemical shift of xenon at each site and $K_{\text{nonspecific}}$ is the strength of the binding interaction at that site. ^{129}Xe chemical shift data in native metmyoglobin solutions are fit to a model that also accounts for the strong specific binding site in native metmyoglobin, yielding an α value of 2–3 ppm/mM. Interestingly, the effect of weak interactions under denaturing conditions is less—$\alpha = 1$ ppm/mM—despite an increased number of potential nonspecific interaction sites upon unfolding.

Here we attempt to develop a more complete characterization of the effects of nonspecific interactions between xenon and proteins on the ^{129}Xe chemical shift in aqueous solution. ^{129}Xe NMR data for xenon dissolved in amino acid, peptide, and protein solutions under both native and denaturing conditions are presented. Comparison of α values for individual amino acids in solution illustrate the importance of molecular properties such as chemical functionality, structure, and charge in determining the ^{129}Xe chemical shift. In solutions of denatured proteins, α has a linear dependence on protein size, thus demonstrating the additivity of diffusion-mediated interactions in aqueous solution. The presence of weak xenon binding sites in cavities and at the surface of native proteins further influences ^{129}Xe chemical shifts in a manner that likely depends on particular features of macromolecular structure. Effects of changes in the xenon solvation shell structure are investigated in solution with varying concentrations of urea. The implications of these findings for the potential use of xenon as a biomolecular probe are considered.

RESULTS AND DISCUSSION

Xenon Interactions in Amino Acid Solutions

A series of ^{129}Xe NMR spectra of xenon (≈11 mM) in 80% H_2O/20% D_2O containing glycine at different concentrations is shown in Fig. 1. The full spectrum (Fig. 1a) contains two peaks—the downfield peak (0 ppm) corresponds to the shift of xenon dissolved in solution, while the upfield peak (≈ −188.6 ppm) corresponds to xenon gas and is used for *in situ* referencing (see Experimental). As the glycine concentration is increased (Figs. 1b, 1c), the solution peak moves downfield, such that the ^{129}Xe shift relative to the ^{129}Xe shift in water ($\delta_{\text{glycine}} - \delta_{\text{water}}$) increases linearly with amino acid concentration. The sharp solution line (typically $\Delta\upsilon \sim 0.05$ ppm) allows accurate determination of the shifts; a linear fit of the data plotted in Fig. 1c yields a value for the slope $\alpha = 0.0043 \pm 0.0001$ ppm/mM. In a similar manner, α values for several amino acids were determined and are listed in Table 1. As seen in Fig. 1c for glycine, alanine, and leucine, all of the amino acids used in these experiments induce ^{129}Xe shifts that are downfield relative to the ^{129}Xe shift in buffer, which indicates that nonspecific interactions between xenon and amino acids deshield the xenon nucleus more than interactions with water alone. Given the dilute solute concentrations for which this effect is observable, deshielding likely occurs through direct xenon–solute interactions which polarize the xenon electron cloud rather than through a solute-induced change in bulk water structure. This supposition is consistent with previous accounts of the deshielding effects of ions in aqueous solution (*25*).

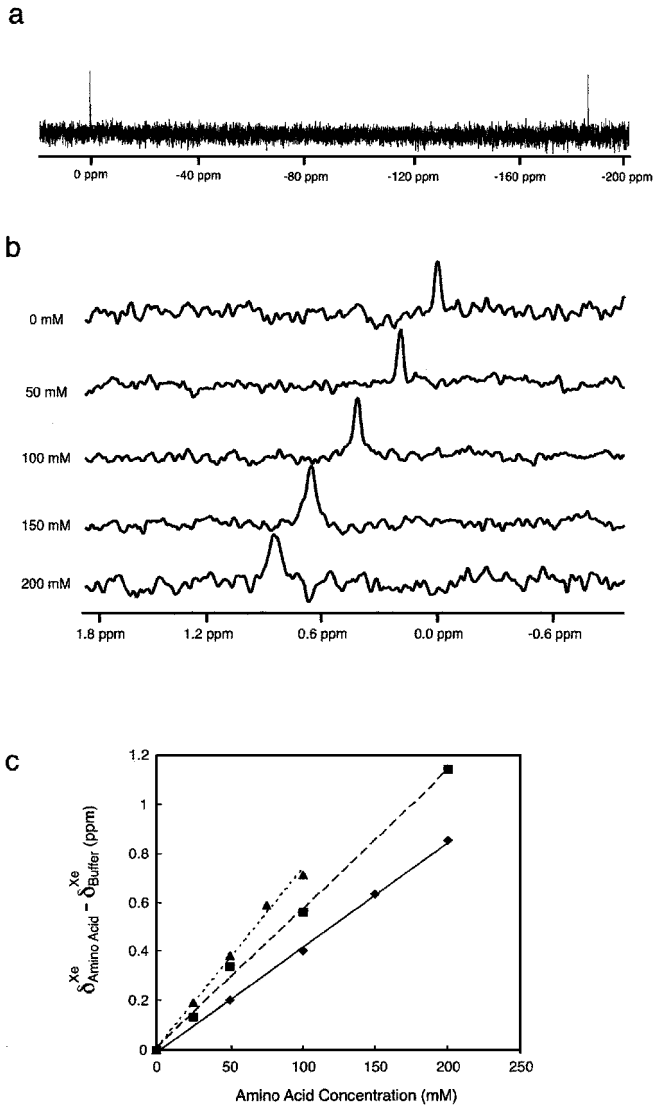

FIG. 1. Effect of glycine on ^{129}Xe NMR chemical shifts of xenon in aqueous solution. (a) Spectrum of xenon alone in 80% H_2O/20% D_2O at a concentration ≈11 mM. The downfield peak (0 ppm) corresponds to solvated xenon, while the upfield signal (≈−188.6 ppm) is due to xenon gas present in a glass capillary tube and is used for in situ referencing. (b) Dissolved xenon resonances in solutions of varying glycine concentration in 80% H_2O/20% D_2O. The ^{129}Xe signal shifts downfield with increasing glycine concentration. (c) Plot of ^{129}Xe chemical shift as a function of amino acid concentration for xenon dissolved in solutions containing glycine (◆), alanine (■), and leucine (▲). Shifts are referenced to the ^{129}Xe chemical shifts of xenon dissolved in 80% H_2O/20% D_2O. Linear fits of the data yields slopes of $\alpha_{glycine} = 0.0042 \pm 0.0001$ ppm/mM, $\alpha_{alanine} = 0.0057 \pm 0.0001$ ppm/mM, and $\alpha_{leucine} = 0.0073 \pm 0.001$ ppm/mM.

The deshielding effects of amino acids resulting from nonspecific xenon–solute interactions can be quantitatively understood in a manner consistent with previous models for ^{129}Xe chemical shifts that consider pairwise van der Waals interactions between xenon and solvent functional groups. In these models, the ^{129}Xe chemical shift is determined by the molar density of functional groups present in the solvent, where the relative deshielding effect of each functional group is related to the strength of the van der Waals interaction between the functional group and xenon (*17, 18, 20*). As predicted by this analysis, the ^{129}Xe chemical shift depends linearly on the mole fraction composition of noninteracting solvent mixtures as the concentrations of functional groups interacting with xenon changes (*18, 27*). We propose that the linear change in the ^{129}Xe chemical shift with the addition of amino acids in aqueous solution is analogously due to changes in functional group concentrations; thus, the overall deshielding of xenon will be due to additive dispersive van der Waals interactions. The trend in α values for the aliphatic and polar amino acids listed in Table 1 supports this conclusion. Studies of xenon in linear functionalized alkanes and alcohols have suggested that the deshielding contributions of methyl and methylene groups are more significant than the contribution of hydroxyl groups due to a larger dispersive interaction energy (*18*). Accordingly, increasing the methyl group concentration in water should result in an increase in the ^{129}Xe chemical shift that reflects the relative Xe–CH_3 and Xe–OH interaction energies. Indeed, the observed increase in α from glycine ($\alpha = 0.0042 \pm 0.0001$ ppm/mM) to alanine ($\alpha = 0.0057 \pm 0.0002$ ppm/mM), which corresponds to the addition of a methyl group, is in agreement with this prediction. It is thus seen that the chemical identity of the amino acid sidechain has a characteristic effect on the ^{129}Xe shift in aqueous solution that is consistent with previous studies in solvent.

TABLE 1
^{129}Xe Deshielding in Amino Acid Solutions

Amino acid	α (ppm/mM)[a] $\times 10^{-3}$	Xenon accessible surface Area (Å^2)[b]
Glycine	4.2 ± 0.1	254
Alanine	5.7 ± 0.2	282
Valine	6.1 ± 0.1	328
Leucine	7.3 ± 0.3	365
Serine	4.5 ± 0.2	301
Threonine	4.6 ± 0.2	320
Tyrosine[c]	7.5 ± 0.8	422
Proline	3.9 ± 0.3	329
Aspartic acid[d]	9 ± 1	347
YPYDVPDYA[d]	38 ± 3	—

[a] Reported α values are the concentration-normalized downfield shifts induced by each amino acid or peptide relative to the ^{129}Xe chemical shift of xenon alone in water. α values were determined from a linear fit of ^{129}Xe chemical shift data of xenon (≈11 mM) dissolved in five solutions of each amino acid or peptide (see Experimental).

[b] Solvent accessible surfaces were calculated with the GRASP software package.

[c] Tyrosine measurements were made in phosphate buffer at pH 11.5 to improve solubility.

[d] Aspartic acid and peptide measurements were made in phosphate buffer at pH 7.0.

Effects of Sidechain Accessibility, Polar Groups, and Charges on ^{129}Xe Deshielding

Further examination of the α values listed in Table 1 reveals the importance of molecular structure and functional group contributions to the ^{129}Xe chemical shift. There exists a positive correlation between the xenon accessible surface area of aliphatic amino acids and the extent of deshielding characterized by the parameter α; such a correlation is indicative of a mechanism of deshielding through van der Waals interactions between xenon and the solute. This trend in aqueous solution is similar to observations previously made for xenon dissolved in organic solvent consisting of different length hydrocarbon chains (18). The polar amino acids are apparent exceptions to the correlation between sidechain size and deshielding. The xenon accessible surface area of serine (301 Å^2) and threonine (320 Å^2) are similar to alanine (282 Å^2) and valine (327 Å^2), but the α values of both amino acids are more comparable to glycine (254 Å^2). This observation suggests that the hydroxyl group contribution to xenon deshielding in aqueous solution is smaller than methyl and methylene groups and is consistent with the relative Xe–CH_3 and Xe–OH interaction energies (18).

The strong deshielding effect of charges in amino acid side chains is reflected by the α for aspartic acid listed in Table 1. Whereas the accessible surface area of aspartic acid (348 Å^2) is comparable to that of leucine (365 Å^2), the α value is significantly greater, indicating that the aspartate anion present at pH 7 considerably influences the ^{129}Xe shift. The zwitterions present in the free amino acid backbone at pH 7 also likely contribute to the α values listed for the amino acids in Table 1. Consequently, one should not expect that the α value of a peptide to correspond exactly to the sum of the α values for the individual amino acids of which the peptide is composed; although the backbone and sidechain functional groups remain accessible to xenon interactions, the formation of peptide bonds removes the significant contribution of backbone ions to ^{129}Xe deshielding. As expected, the experimental value of α for the peptide YPYDVPDYA ($\alpha_{exp} = 0.038 \pm 0.003$) was found to be less than the sum of the individual amino acid contributions based on the values in Table 1 ($\alpha_{calc} = 0.061 \pm 0.005$).

Interactions of Xenon in Denatured Protein Solutions

The effects of van der Waals interactions and molecular structure on the ^{129}Xe chemical shift observed in aqueous solutions of amino acids provide a framework for characterizing the effects of nonspecific interactions between xenon and proteins. Figure 2 shows ^{129}Xe chemical shift data for titrations of hen egg white lysozyme and bovine serum albumin (BSA) under both native and denaturing conditions at a xenon concentration of ≈11 mM. As previously observed in myoglobin solution (*13*), nonspecific interactions between xenon and these proteins induce a downfield shift relative to the shift of xenon in aqueous buffer alone ($\delta_{buffer} = 0$ ppm). This trend is consistent with the linear change in the concentration of functional groups interacting with xenon upon addition of protein to water and the deshielding effect of this change as observed in amino acid solutions. Insofar as denatured proteins lack structured internal cavities that bind xenon, their α values depend only on diffusion-mediated interactions with xenon. Accordingly, α should increase with denatured protein size as the concentration of accessible functional groups increases. Figure 3 shows the α value of the peptide YPYDVPDYA and the proteins lysozyme, RNaseA, proteinase K, and BSA under native and denaturing conditions. The α values for the peptide and denatured proteins have a linear dependence on the number of amino acids in the protein sequence, thus confirming the additivity of deshielding effects due to dispersive van der Waals interactions. Slight discrepancies may exist because of differences in specific amino acid composition, but we have measured the average α value for a denatured protein to equal ≈0.005 ppm/mM per amino acid. A notable exception to the linear trend shown in Fig. 3 is the α value previously reported for denatured metmyoglobin (*13*), which is greater than predicted. However, the presence of the iron heme in solution may account for the increased deshielding of xenon; our preliminary data suggest that the addition of heme alone to 6M urea solution results in a substantial downfield shift of the ^{129}Xe resonance.

Interactions of Xenon in Native Proteins: Effects of Weak Binding Sites

Given the importance of functional group accessibility to xenon in determining the overall deshielding, consideration of diffusion-mediated xenon–protein interactions alone would predict that α values for denatured proteins should be consistently greater than α values of native proteins where amino acid sidechains are buried within a core. However, as observed in the case of BSA (Fig. 2), proteinase K, and previously in myoglobin (*13*), α values of proteins can be greater under native conditions than under denaturing conditions. Furthermore, as seen in Fig. 3, the α values of native proteins do not show a simple dependence on the number of amino acids in the protein sequence; this behavior suggests contributions to α from effects other than diffusion-mediated interactions. A more detailed model for how native proteins affect ^{129}Xe chemical shifts must account for the possibility of cavities within the macromolecular structure or surface sites which preferentially interact with xenon. Indeed, examples of multiple xenon binding sites in proteins have been observed in crystal structures of myoglobin, lysozyme, and several serine proteases (*28, 29*). In all cases except the primary binding site in myoglobin, these binding interactions are weak enough so that the fraction of total xenon in solution occupying cavity or surface sites is small. Accordingly, the presence of such binding sites results in a change in the overall ^{129}Xe chemical shift that is directly proportional to protein concentration, and α for a protein can be considered as the sum of a large number of weak binding interactions consisting of both cavity sites within the native structure and diffusion-mediated

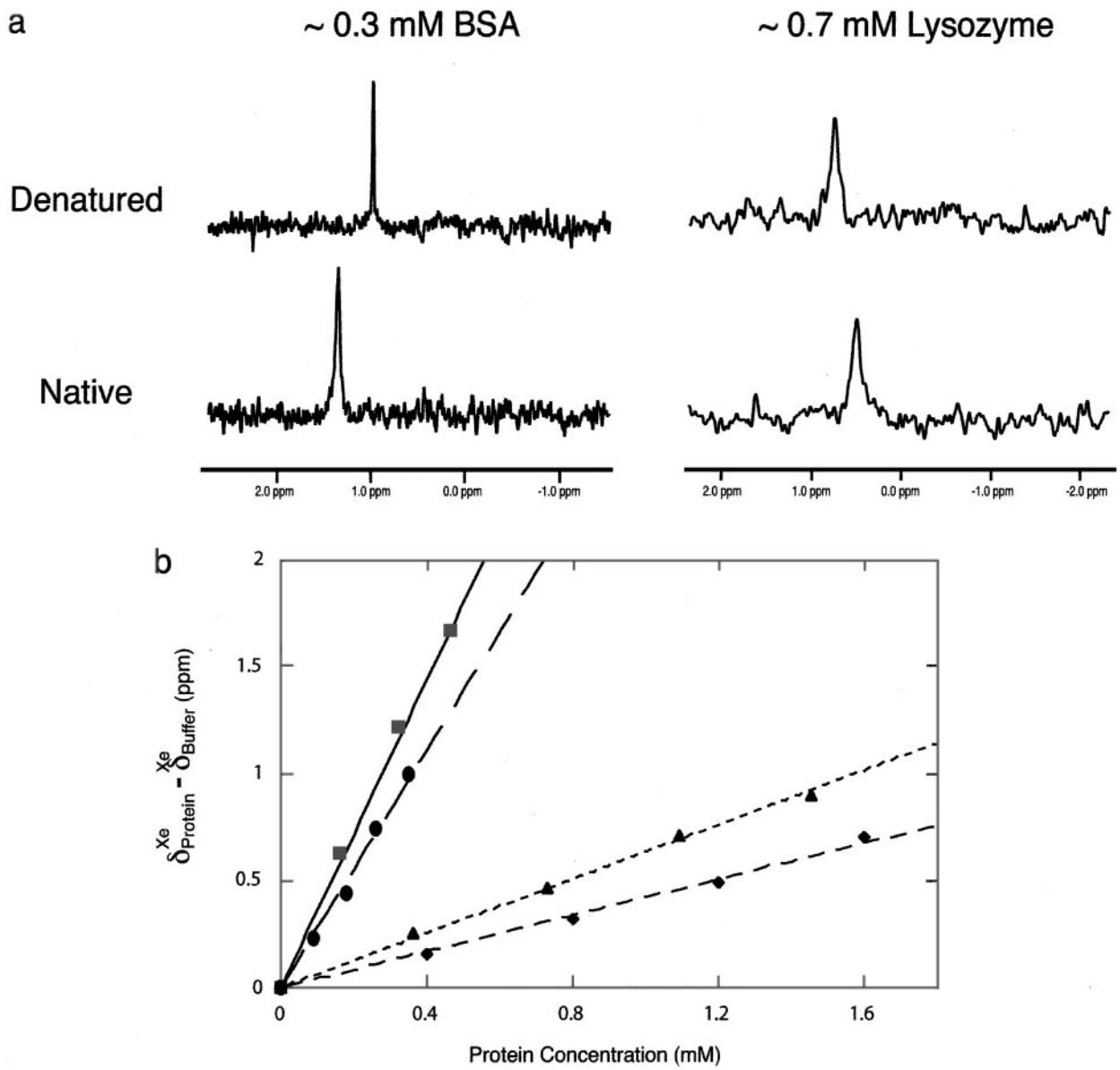

FIG. 2. Effects of lysozyme and bovine serum albumin (BSA) on ^{129}Xe chemical shifts in aqueous solution. (a) ^{129}Xe NMR spectra of xenon ($\approx$11 mM) dissolved in solutions of $\sim$0.3 mM BSA and $\sim$0.7 mM lysozyme under native (phosphate buffer pH 7.0) and denaturing conditions (citrate bufer pH 2.9, 6 M urea). All ^{129}Xe chemical shifts are downfield relative to the shift of xenon alone in each buffer ($\delta_{buffer} = 0$ppm). The extent of xenon deshielding in native protein solution relative to denatured protein solution differs for the two proteins; this difference reflects the presence of effects from weak binding sites that are particular to native protein structure.(b) ^{129}Xe chemical shifts of $\approx$11 mM xenon dissolved in solutions of native lysozyme (◆), denatured lysozyme (▲), native BSA (■), and denatured BSA (●). Chemical shift values are reported relative to the value for xenon alone in buffer solution. Linear fits of the data yields slopes of $\alpha_{lysozyme} = 0.43 \pm 0.01$ ppm/mM and $\alpha_{BSA} = 3.48 \pm 0.04$ ppm/mM under native conditions at pH 7.0 and $\alpha_{lysozyme} = 0.62 \pm 0.02$ ppm/mM and $\alpha_{BSA} = 2.87 \pm 0.10$ ppm/mM under denaturing conditions at pH 2.9.

interactions between xenon and accessible protein functional groups.

Whereas denaturation always increases the number of deshielding dispersive interactions, proteins such as BSA that have $\alpha_{denatured} < \alpha_{native}$ must have a strong downfield contribution to α from cavity sites present only in the native structure. The presence of such cavities in BSA is supported by the fact that the ^{129}Xe spin-lattice relaxation time is longer in blood plasma that also contains the drug flucloxacillin, which binds specifically to BSA (*30*). Conversely, proteins such as lysozyme with $\alpha_{denatured} > \alpha_{native}$ have an overall upfield contribution from cavity sites or a downfield contribution from a small number of such sites that is modest compared to that from the increase of dispersive interactions upon denaturation. Specific xenon binding sites in hen egg-white lysozyme have been observed by x-ray crystallography (*29*). The direction of

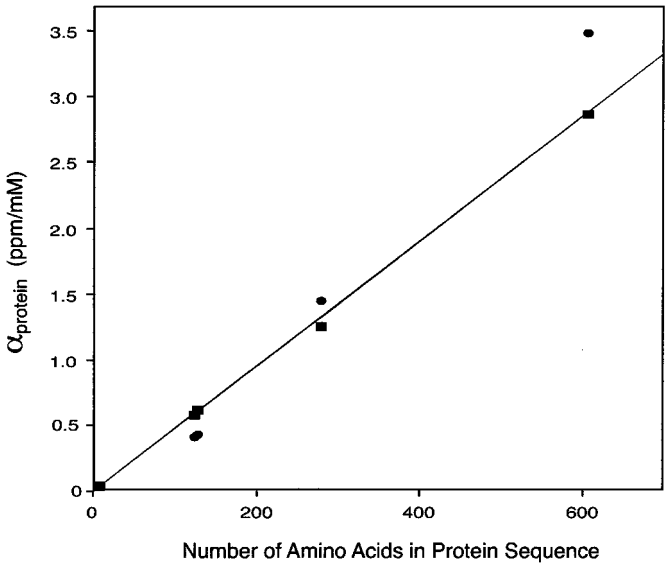

FIG. 3. Values of the parameter α (solute concentration dependence of the ^{129}Xe chemical shift) for the peptide YPYDVPDYA and the proteins hen egg white lysozyme (129 amino acids), RNaseA (124), proteinase K (279), and BSA (607) under native (●) and denaturing (■) conditions as a function of the number of amino acids in the protein sequence. The linear dependence of α values for denatured proteins on protein size demonstrates the additivity of xenon deshielding due to diffusion-mediated interactions in solution; a linear fit yields a slope $\approx$0.005 ppm/mM per amino acid, reflecting the average value of α for an amino acid in a protein.

the shift contribution from cavity sites is determined by the structure of the cavity and is likely consistent with observations of xenon shifts in clathrates, zeolites, and nanochannels (*22–24*).

Xenon Solvation Shell Structure in Aqueous Solution

The above account of ^{129}Xe chemical shifts in amino acid, peptide, and protein solutions ignores any effects the cosolute may have on the structure of the solvation shell around xenon. The local water structure around xenon results in a ^{129}Xe chemical shift in pure water which is further downfield than anticipated by a pairwise van der Waals interaction model (*7, 18*). However, the introduction of additional van der Waals interactions between xenon and amino acids leads to further relative deshielding that is reasonably consistent with a functional group analysis alone. This observation suggests that the structure of the xenon solvation shell in water effectively remains intact in the dilute conditions used in these experiments. In order to examine the effects of high solute concentrations on the ^{129}Xe chemical shift, ^{129}Xe NMR spectra were acquired of $\approx$11 mM xenon dissolved in urea solutions up to 8 M. As seen in Fig. 4, the behavior of the measured shifts with increasing urea concentration is quite different from that in dilute amino acid and protein solutions—the ^{129}Xe chemical shift remains nearly constant at low urea concentration and moves upfield relative to water at urea concentrations greater than $\sim$1 M.

A similar trend in ^{129}Xe chemical shift data has been observed in mixtures of water with cosolvents such as alcohols, dioxane, and acetonitrile (*31*). At low mole fractions of cosolvent, the ^{129}Xe chemical shift remains constant or moves linearly downfield; beyond a certain mole fraction, the shift moves upfield until it reaches the limiting shift in pure cosolvent. The behavior of these solutions in the dilute limit is consistent with the addition of solute that either does (in the case of alcohols and dioxane) or does not (in the case of urea and acetonitrile) change significantly the van der Waals deshielding of xenon. The upfield influence on the ^{129}Xe chemical shift cannot be explained by changes in functional group concentrations that affect deshielding; alternatively, the upfield behavior suggests that the addition of large amounts of urea or cosolvent changes the unique effect of water structure on the overall shift. Thus, the relative upfield chemical shift of xenon in concentrated urea solution likely reflects a change in the structure of the xenon solvation shell from that in pure water. This sensitivity to solvent shell structure and the simplicity of modeling xenon as a hydrophobic solvent encourages the application of ^{129}Xe NMR in studying the effects of denaturant and the mechanism of protein denaturation.

Outlook for the Use of Xenon as a Biomolecular Probe

Observations of ^{129}Xe NMR signals in aqueous solutions of amino acids, peptides, and proteins under both native and denaturing conditions have elucidated the contributions of chemical functionality, charge, solute accessibility, and macromolecular structure to the ^{129}Xe chemical shift. The ability to predict how changes of these properties affect ^{129}Xe chemical shifts may allow for the use of xenon as a biomolecular probe. For example, the dependence of α on accessible protein surface area may be

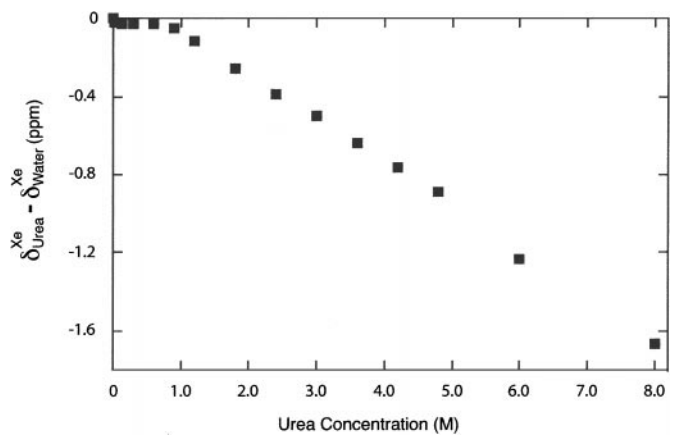

FIG. 4. ^{129}Xe chemical shifts of xenon ($\approx$11 mM) dissolved in 80% H_2O/20% D_2O as a function of added urea. Chemical shift values are reported relative to the value for xenon alone in 80% H_2O/20% D_2O. The upfield trend at high urea concentration is consistent with a change in the contribution of solvent shell structure to the ^{129}Xe chemical shift.

useful in identifying the formation of protein–protein interfaces. Amino acid side chains that were previously exposed to solvent become inaccessible to xenon upon formation of an interface; accordingly, protein deshielding due to diffusion-mediated interactions should decrease. The magnitude of this decrease in α quantifies how much surface area is buried at the interface. The dependence of α on particular structural features of native proteins such as the existence of xenon cavity sites and the amino acid composition of the protein surface suggests that native state conformational changes may be detected by an observable change in α. The observation of the effect of a change in α upon protein denaturation already demonstrates the use of ^{129}Xe chemical shifts to sense a change in protein structure upon modifying solution conditions. In addition, we have attained evidence that the shift is sensitive to the different native state conformations of a sugar binding protein (*32*). Considering the sharp ^{129}Xe resonance lines of xenon in these solutions, one can contemplate assaying conformational changes that result in $\Delta\alpha \sim 1$ ppm/mM at protein concentrations down to $\sim$10 μM. The fact that the ^{129}Xe chemical shift is highly sensitive to changes in macromolecular properties even in the absence of strong specific binding interactions suggests that xenon can be used as a general probe of biomolecular systems.

EXPERIMENTAL

All chemicals were purchased from Sigma and used without further purification. Amino acid and peptide samples used in titrations were typically prepared by dissolving a known mass of solid powder in water or 100 mM phosphate buffer (pH 7.0) containing 20% D_2O, to create a 25–200 mM stock solution. Native protein and peptide solutions were prepared by dissolving lyophilized powder in 100 mM phosphate buffer (pH 7.0) containing 20% v/v D_2O. Denatured protein solutions were prepared by dissolving lyophilized powder in 100 mM citrate, 6 M urea, and 5 mM DTT (RNaseA only) (pH 2.9) containing 20% v/v D_2O. Concentrations of protein and peptide stock solutions ranged from 0.35 to 2.0 mM and 5.3 mM, respectively, as determined by the absorbance of 280-nm UV light using $\varepsilon_{\mathrm{YPYDVPDYA}} = 4470\ \mathrm{M^{-1}\ cm^{-1}}$, $\varepsilon_{\mathrm{lysozyme}} = 37{,}970\ \mathrm{M^{-1}\ cm^{-1}}$, $\varepsilon_{\mathrm{BSA}} = 42{,}925\ \mathrm{M^{-1}\ cm^{-1}}$, $\varepsilon_{\mathrm{RNaseA}} = 9440\ \mathrm{M^{-1}\ cm^{-1}}$, and $\varepsilon_{\mathrm{proteinaseK}} = 36{,}560\ \mathrm{M^{-1}\ cm^{-1}}$ (33).

Chemical shift measurements were made as previously described using 80% enriched ^{129}Xe (Isotec) that was loaded into a medium-walled NMR tube (Wilmad, Buena, NY) adapted with a screw cap to hold the gas (*13*). Samples were degassed through freeze–thaw cycles and evacuated prior to loading $\approx$2.5 atm xenon; gas pressures were confirmed with a gauge upon loading and rechecked upon subsequent recovery of the gas after each experiment. Assuming the concentration of xenon in water depends linearly on pressure, with a slope of 4.4 mM/atm (*34*), we determine a xenon concentration of $\approx$11 mM in solution. A reasonably consistent pressure ($\pm$0.2 atm) was necessary as the ^{129}Xe chemical shift in water changes $\sim$0.01 ppm per mM xenon in solution. Samples were gently agitated and allowed to equilibrate before acquisition of data with either a Bruker AMX 600 MHz or a Varian Inova 300 MHz spectrometer. A sealed glass capillary tube filled with $\sim$5 atm of xenon gas was included in each sample as a standard reference. The ^{129}Xe chemical shifts in water, phosphate buffer (pH 7.0), and citrate buffer with 6 M urea (pH 2.9) were typically 188.6, 189.1, and 187.0 ppm downfield from this gas reference and were sensitive to salt concentration and mole fraction D_2O.

In each solution, the ^{129}Xe chemical shift was determined from the highest point of the solution resonance peak (the estimated accuracy of chemical shift determination is $\sim$0.01 ppm) and referenced to the chemical shift of xenon in buffer alone (i.e., $\delta_{\mathrm{buffer}} = 0$ ppm). The values of α for each titration were determined from linear fits of chemical shift measurements in solutions at five different amino acid or protein concentrations that were generated by the dilution of initial stock solutions. The concentrations of solute were high enough so that the difference in ^{129}Xe chemical shifts between points in titrations ($>$0.2 ppm) were large compared to the uncertainty in the measurement due to the xenon concentration and resonance linewidth ($\sim$0.01 ppm). Linear fits of the titration data yield standard errors such that all differences between the reported α values (except between threonine and serine) are statistically significant with a confidence of $>$95%. The xenon accessible surface areas of amino acids were determined using the software GRASP (probe radius 2.0Å) and PDB coordinate files from the Hetero-Compond Information Center, Uppsala (http://xray.bmc.uu.se/hicup); these coordinate files lacked an oxygen on the backbone carboxylate group.

ACKNOWLEDGMENTS

The authors thank Dr. David King for providing the YPYDVPDYA peptide, Tom Lawhead for his expert glassblowing and advice, S.Y. Lee for assistance in using GRASP, and I.E. Dimitrov for useful discussions regarding the manuscript. S.M.R. and M.M.S. acknowledge the National Science Foundation for predoctoral fellowships. This work was supported by the Director, Office of Energy Research, Office of Basic Energy Sciences, Materials Sciences Division, Physical Biosciences Division, of the U.S. Department of Energy under Contract DE-AC03-76SF00098.

REFERENCES

1. T. Ito and J. Fraissard, 129-Xe NMR study of xenon adsorbed on Y zeolites, *J. Chem. Phys.* **76,** 5225–5229 (1982).
2. J. Jokisaari, NMR of noble gases dissolved in isotropic and anisotropic liquids, *Prog. Nucl. Magn. Reson. Spectrosc.* **26,** 1–26 (1993).
3. C. I. Ratcliffe, Xenon NMR, *Annu. Rep. NMR Spectrosc.* **36,** 124–208 (1998).
4. J. Bonardet, J. Fraissard, A. Gédéon, and M. Springuel-Huet, Nuclear magnetic resonance of physisorbed 129-Xe used as a probe to investigate porous solids, *Catal. Rev. Sci. Eng.* **41,** 115–225 (1999).
5. B. M. Goodson, L. Kaiser, and A. Pines, NMR and MRI of laser-polarized noble gases in molecules, materials, and medicine, *Proc. Int. Sch. Phys. "Enrico Fermi"* **139,** 211–260 (1999).

6. T. G. Walker and W. Happer, Spin-exchange optical pumping of noble-gas nuclei, *Rev. Mod. Phys.* **69,** 629–642 (1997).
7. K. W. Miller, N. V. Reo, A. J. Schoot Uiterkamp, D. P. Stengle, T. R. Stengle and K. L. Williamson, Xenon NMR: Chemical shifts of a general anesthetic in common solvents, proteins, and membranes, *Proc. Natl. Acad. Sci. U.S.A.* **78,** 4946–4949 (1981).
8. R. F. Tilton, Jr., and I. D. Kuntz, Jr., Nuclear magnetic resonance studies of xenon-129 with myoglobin and hemoglobin, *Biochemistry* **21,** 6850–6857 (1982).
9. S. McKim and J. F. Hinton, Evidence of xenon transport through the gramicidin channel: A 129-Xe NMR study, *Biochim. Biophys. Acta* **1193,** 186–198 (1994).
10. C. R. Bowers, V. Storhaug, C. E. Webster, J. Bharatam, A. Cottone, R. Gianna, K. Betsey, and B. J. Gaffney, Exploring surfaces and cavities in lipoxygenase and other proteins by hyperpolarized xenon-129 NMR, *J. Am. Chem. Soc.* **121,** 9370–9377 (1999).
11. J. Wolber, A. Cherubini, M. O. Leach, and A. Bifone, Hyperpolarized 129-Xe NMR as a probe for blood oxygenation, *Magn. Reson. Med.* **43,** 491–496 (2000).
12. E. Locci, M. Casu, G. Saba, A. Lai, M. Luhmer, J. Reisse, and K. Bartik, personal communication.
13. S. M. Rubin, M. M. Spence, B. M. Goodson, D. E. Wemmer and A. Pines, Evidence of nonspecific surface interactions between laser-polarized xenon and myoglobin in solution, *Proc. Natl. Acad. Sci. U.S.A.* **97,** 9472–9475 (2000).
14. C. J. Jameson, A. K. Jameson, and S. Cohen, Temperature and density dependence of Xe-129 chemical shift in xenon gas, *J. Chem. Phys.* **59,** 4540–4546 (1973).
15. B. F. Chmelka, D. Raftery, A. V. McCormick, L. C. de Menorval, R. D. Levine, and A. Pines, Measurement of xenon distribution statistics in Na-A zeolite cavities, *Phys. Rev. Lett.* **66,** 580–583 (1991).
16. A. D. Buckingham, T. Schaefer, and W. G. Schneider, Solvent effects in nuclear magnetic resonance spectra, *J. Chem. Phys.* **32,** 1227–1233 (1960).
17. Y. H. Lim and A. D. King, NMR chemical shifts of Xe-129 dissolved in liquid N-alkanes and their mixtures, *J. Phys. Chem.* **97,** 12,173–12,177 (1993).
18. M. Luhmer and K. Bartik, Group contribution analysis of xenon NMR solvent shifts, *J. Phys. Chem. A* **101,** 5278–5283 (1997).
19. F. H. A. Rummens, On the use of the Bayliss–McRae dispersion model in NMR solvent effects, *Chem. Phys. Lett.* **31,** 596–598 (1975).
20. M. Luhmer, A. Dejaegere, and J. Reisse, Interpretation of the solvent effect on the screening constant of Xe-129, *Magn. Reson. Chem.* **27,** 950–952 (1989).
21. J. A. Ripmeester and D. W. Davidson, Xe-129 nuclear magnetic resonance in the clathrate hydrate of xenon, *J. Mol. Struct.* **75,** 67–72 (1981).
22. J. Fraissard and T. Ito, 129-Xe N.M.R. Study of adsorbed xenon: A new method for studying zeolites and metal-zeolites, *Zeolites* **8,** 350–361, (1988).
23. J. A. Ripmeester, C. I. Ratcliffe, and J. S. Tse, The nuclear magnetic resonance of Xe-129 trapped in clathrates and some other solids, *J. Chem. Soc. Faraday Trans.* **84,** 3731–3745 (1988).
24. P. Sozzani, A. Comotti, R. Simonutti, T. Meersmann, J. W. Logan, and A. Pines, A porous crystalline molecular solid explored by hyperpolarized xenon, *Angew. Chem. Int. Ed. Eng.* **39,** 2695–2698 (2000).
25. S. McKim and J. F. Hinton, Xe-129 NMR spectroscopic investigation of the interaction of xenon with ions in aqueous solution, *J. Magn. Reson. A* **104,** 268–272 (1993).
26. K. Bartik, M. Luhmer, S. J. Heyes, R. Ottinger, and J. Reisse, Probing molecular cavities in alpha-cyclodextrin solutions by xenon NMR, *J. Magn. Reson. B* **109,** 164–168 (1995).
27. T. R. Stengle, S. M. Hosseini, and K. L. Williamson, NMR shifts of xenon in mixed aprotic solvents: A probe of liquid structure, *J. Solution. Chem.* **15,** 777–789 (1986).
28. R. F. Tilton, Jr., I. D. Kuntz, Jr., and G. A. Petsko, Cavities in proteins: Structure of a metmyoglobin–xenon complex solved to 1.9 Å, *Biochemistry* **23,** 2849–2857 (1984).
29. T. Prangé, M. Schiltz, L. Pernot, N. Colloc'h, S. Longhi, W. Bourget, and R. Fourme, Exploring hydrophobic sites in proteins with xenon and krypton, *Struct. Funct. Genet.* **30,** 61–73 (1998).
30. J. Wolber, A. Cherubini, A. S. K. Dzik-Jurasz, M. O. Leach, and A. Bifone, Spin-lattice relaxation of laser-polarized xenon in human blood, *Proc. Natl. Acad. Sci. U.S.A.* **96,** 3664–3669 (1999).
31. T. R. Stengle, S. M. Hosseini, H. G. Basiri, and K. L. Williamson, NMR chemical shifts of xenon in aqueous solutions of amphiphiles: A new probe of the hydrophobic environment, *J. Solution. Chem.* **13,** 779–787 (1984).
32. C. N. Pace, F. Vajdos, L. Fee, G. Grimsley, and T. Gray, How to measure and predict the molar absorption coefficient of a protein, *Protein Sci.* **4,** 2411–2423 (1995).
33. H. L. Clever, "Solubility Data Series," Pergamon, New York (1979).
34. S. M. Rubin, M. M. Spence, I. E. Dimitrov, E. J. Ruiz, A. Pines, and D. E. Wemmer, submitted for publication.